

Clusters, columns, and lamellae—minimum energy configurations in core softened potentials

Gernot J. Pauschenwein and Gerhard Kahl

Received 11th April 2008, Accepted 1st May 2008

First published as an Advance Article on the web 20th May 2008

DOI: 10.1039/b806147e

We give evidence that particles interacting *via* the simple, radially symmetric square-shoulder potential can self-organise in highly complex, low-symmetry lattices, thereby forming clusters, columns, or lamellae; only at high pressure are compact, high-symmetry structures observed. Our search for these ordered equilibrium structures is based on ideas of genetic algorithms, a strategy that is characterised by a high success rate. A simple mean-field type consideration complements these findings and locates in a semi-quantitative way the cross-over between the competing structures.

“One of the continuing scandals in the physical sciences is that it remains in general impossible to predict the structure of even the simplest crystalline solids from a knowledge of their chemical composition.”¹ Even nowadays, twenty years later, this statement is still valid and it applies equally well to the case where the *physical* properties of the system, *e.g.*, in terms of its inter-particle potential, are known. Indeed, in many problems of hard and soft condensed matter theory a powerful tool that is able to *predict* the ordered equilibrium structures of a system in a reliable way is badly missing. This applies in particular to soft matter systems where particles are able to self-organise in a broad variety of unexpected and often very exotic ordered structures: micellar and inverse micellar structures,^{2,3} spirals,⁴ chains and layers,^{3,5} and cluster phases^{6,7} are a few examples.

During the past decades several strategies have been proposed to find the energetically most favourable particle arrangements of a system. Apart from conventional approaches that rely on intuition, experience, or plausible arguments when selecting candidates for ordered equilibrium structures, there are more sophisticated approaches such as simulated annealing,⁸ basin hopping,⁹ or metadynamics.¹⁰ However, all these strategies are affected by different sorts of deficiencies which can significantly reduce their success rates.

In recent years convincing evidence has been given that search strategies based on ideas of genetic algorithms (GAs) are able to provide a significant break-through to solve this problem. Generally speaking, GAs are strategies that use key ideas of evolutionary processes, such as survival of the fittest, recombination, or mutation, to find optimal solutions for a problem.¹¹ The wide spectrum of obviously successful applications in different fields of condensed matter physics unambiguously demonstrates their flexibility, reliability, and efficiency: among these are laser pulse control,¹² protein folding,¹³ or cluster formation.¹⁴ In contrast, attempts to apply GAs in the search for ordered equilibrium structures in condensed matter theory were realised considerably later. While the first application

probably dates back to 1999¹⁵ their widespread use in hard matter theory was pioneered by Oganov and Glass¹⁶ only recently, where they have meanwhile become a standard tool: a wide spectrum of successful applications ranging from geophysical to technologically relevant problems gives evidence of the power and the flexibility of this approach (for an overview see ref. 16). In *soft* condensed matter theory the usage of these search strategies is still in its infancy. First applications to find minimum energy configurations (MECs) of soft systems have, nevertheless, unambiguously documented the power of the algorithm: successful examples are the identification of exotic lattice structures and cluster phases for particular soft systems,^{7,17} or of complex, ordered arrangements of monolayers of binary dipolar mixtures.¹⁸ All these investigations mentioned above give evidence that GA-based search strategies have an extremely high success rate.

In this contribution we consider a simple soft model system, *i.e.*, a square-shoulder system, and show that the GA is an efficient and reliable tool to identify even highly complex MECs in soft matter systems. We discover an overwhelming and undoubtedly unexpected wealth of ordered MECs, which comprise clusters, columns, lamellae, as well as compact structures. The simple shape of the potential allows an easy geometric interpretation of the system's strategies to form MECs in terms of overlapping shoulders, a nice feature that is not available in systems with continuous potentials. We find evidence that the success rate of our algorithm must be close to 100%.

The square-shoulder system is the simplest representative in the class of the so-called core-softened potentials (for references see ref. 19). Despite their innocent looking potentials these systems are characterised by a host of surprising properties, such as water-like anomalies^{19,20} or a rich wealth in the occurring structures, investigated in detail in two-dimensional systems.^{3,18} The potential $\Phi(r)$ of the square-shoulder system,

$$\Phi(r) = \begin{cases} \infty & r \leq \sigma \\ \varepsilon & \sigma < r \leq \lambda\sigma, \\ 0 & \lambda\sigma < r \end{cases} \quad (1)$$

consists of an impenetrable core of diameter σ with an adjacent, repulsive, step-shaped shoulder of height ε and width $\lambda\sigma$. For the aims of the present contribution it represents the ‘quintessential’ test system.²¹ Further, we introduce the number-density $\varrho = N/V$, N and V being the number of particles and the volume, respectively.

However we also point out that the square-shoulder system is not only of purely academic interest: it represents a reasonable model system for colloidal particles with a core-corona architecture, as, for instance, has been given evidence for in ref. 22. There the authors determine *via* self-consistent field calculations the effective interactions between polymer-grafted colloidal particles; for particular system parameters these closely resemble the interaction of a square

Center for Computational Materials Science and Institut für Theoretische Physik, Technische Universität Wien, Wiedner Hauptstraße 8-10, A-1040 Wien, Austria

shoulder system with $\lambda \approx 2$. Depending on the grafting density of the polymers and/or the quality of the solvent these interactions can be tuned, a feature which is very useful in industrial applications.

The MECs for this system have been identified *via* a GA-based search strategy in the NPT ensemble. For details of the encoding of the individuals (= lattices) and of the reproduction mechanism we refer to ref. 23. The quality of an individual \mathcal{S} is measured *via* the fitness function $f(\mathcal{S})$, for which we have chosen $f(\mathcal{S}) = \exp\{-[G(\mathcal{S}) - G_0]/G_0\}$. Since our investigations are restricted to the case $T = 0$, the Gibbs free energy, $G(\mathcal{S})$, reduces at a given pressure P to $G = U + PV$, U being the lattice sum; G_0 is the Gibbs free energy of a reference structure. Significant extensions of the search strategy were required due to the impenetrable core: as a consequence of the highly stochastic character of GAs, the algorithm will propose with a high probability lattices where the cores of the particles overlap: such configurations are unphysical and thus useless. A more *quantitative* investigation reveals that the physically relevant lattices (characterised by non-overlapping cores of the particles) populate only a highly porous subset of the search space.²⁴

To overcome this problem a suitable modification is urgently required, which guarantees that unphysical configurations are excluded *a priori* so that only lattices with non-overlapping cores are created. Such a strategy has been developed and will be outlined briefly. We start for simplicity with a simple lattice, described *via* a set of linearly independent vectors \mathbf{a}_1 , \mathbf{a}_2 , and \mathbf{a}_3 . In order to satisfy our expectations, they have to meet several requirements. First, the vectors are chosen such that $|\mathbf{a}_1| \leq |\mathbf{a}_2| \leq |\mathbf{a}_3|$, where $|\mathbf{a}_1|$ represents the shortest possible distance between lattice sites. Then, \mathbf{a}_2 is selected so that $|\mathbf{a}_2|$ is either equal to $|\mathbf{a}_1|$ or represents the second smallest distance encountered between two lattice points. Finally, the third vector, \mathbf{a}_3 , is chosen so that $|\mathbf{a}_3|$ satisfies a similar relation with respect to $|\mathbf{a}_2|$. Of course, the choice of the $\{\mathbf{a}_i\}$ is not unique. If we are able to construct a lattice so that *a priori* $|\mathbf{a}_1| \geq \sigma$, then it is guaranteed by construction that the particles will not overlap. We have succeeded in developing a formalism that is able to create vectors $\{\mathbf{a}_i\}$, that satisfy the above requirements. These constraints led to inequalities between the Cartesian components of the vectors; these lengthy relations along with a detailed explanation of the algorithm will be described elsewhere.²⁵ In non-simple lattices overlap can also be caused by the basis particles. Let us assume that the underlying *simple* lattice satisfies above requirements. Then we calculate all the distances between the particles of this cell and all particles located in the 26 neighbouring cells. Let l_0 be the smallest among these distances; if $l_0 < |\mathbf{a}_1|$, then the vectors $\{\mathbf{a}_i\}$ are scaled by a factor $|\mathbf{a}_1|/l_0$, which guarantees that in the entire lattice no particle overlap will occur.

Thermodynamic properties will be presented in standard reduced units: $q^* = q\sigma^3$, $P^* = P\sigma^3/\epsilon$, $U^* = U/(N\epsilon)$, and $G^* = G/(N\epsilon) = U^* + P^*/q^*$. The simple shape of the potential allows us to simplify the search considerably: since for a fixed particle configuration U^* (counting the number of overlapping coronas) is constant, $G^* = U^* + P^*/q^*$ is a straight line of slope $1/q^*$ in the (G^*, P^*) -diagram. The limiting MECs at low and high pressure are easily identified as close-packed spheres, either with diameter $\lambda\sigma$ (corresponding to a slope $1/q_{\min}^* = \lambda^3/\sqrt{2}$) or with diameter σ (corresponding to a slope $1/q_{\max}^* = 1/\sqrt{2}$)—*cf.* Fig. 1. Any other MEC occurring in this system is characterised by a line of slope $1/q^*$, satisfying $1/q_{\min}^* > 1/q^* > 1/q_{\max}^*$. Thus $G^* = G^*(P^*)$ is a sequence of straight lines. In a first step we determine in the (G^*, P^*) -diagram the intersection point of the two limiting straight lines mentioned above and

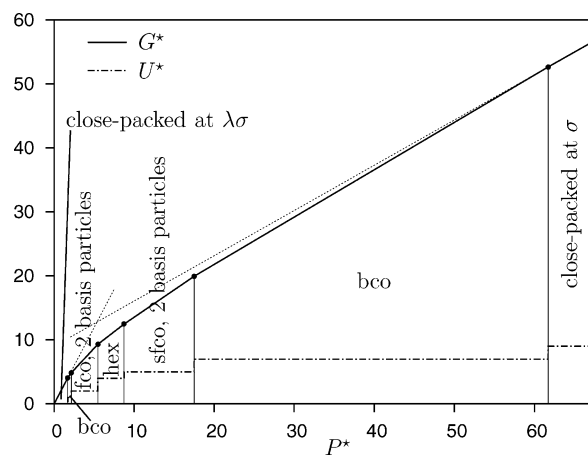


Fig. 1 G^* and U^* as functions of P^* for the square-shoulder system, $\lambda = 1.5$. The dotted lines indicate low- and high-pressure limiting cases of MECs (see text).

launch for this P^* -value a GA-search. This leads to a new MEC, characterised by a lower G^* -value, a density q^* , and thus a new straight line of slope $1/q^*$. Intersecting this line with the previous lines and iterating this strategy, the entire pressure-range can be investigated in an extremely efficient way. From the economic point of view this systematic procedure is very attractive; but it has two additional advantages: (i) there is no risk to ‘forget’ MECs which easily occurs when working on a finite P^* -grid; and (ii) it avoids a characteristic drawback of GAs that tend to fail in the vicinity of state points that are characterised by competing structures; in the present approach these transition points are determined *exactly* *via* the intersection of two straight lines.

At each of the intersection points, 1000 to 3000 independent GA-runs with 700 generations, each consisting of 500 individuals, have been performed. Up to twelve particles per unit cell were considered, a number which offers the system sufficient possibilities to form even highly complex structures. Bearing all this in mind, we are confident that the sequence of MECs which we present in the following is complete.

We have considered three values of λ , corresponding to small ($\lambda = 1.5$), intermediate ($\lambda = 4.5$), and long ($\lambda = 10$) shoulder width. For the first case, G^* and U^* , as functions of P^* , are presented in Fig. 1. G^* is, as mentioned above, a sequence of straight lines, while the energy levels of U^* are rational numbers, given by the number of overlapping coronas per particle. For $\lambda = 1.5$, seven MECs can be identified (*cf.* acronyms in Fig. 1). At low pressure a columnar structure is identified, while for larger P^* -values, the relatively short corona width allows only compact structures.

For $\lambda = 4.5$, the considerably broader corona offers the system a large variety of strategies to form MECs. Their total number amounts to 33 (*cf.* Fig. 2) which can be grouped with increasing pressure into four structural archetypes: cluster phases, columnar structures, lamellar phases, and, finally, compact structures (see also Fig. 4). At low pressure the system forms cluster crystals, *i.e.*, periodic structures where the lattice points are populated by clusters of particles. A closer analysis reveals a strong interplay between the cluster shape and the cell geometry in the sense that overlaps of coronas of neighbouring clusters are avoided. Inside the clusters, which contain up to eight particles, the cores are in direct contact. For

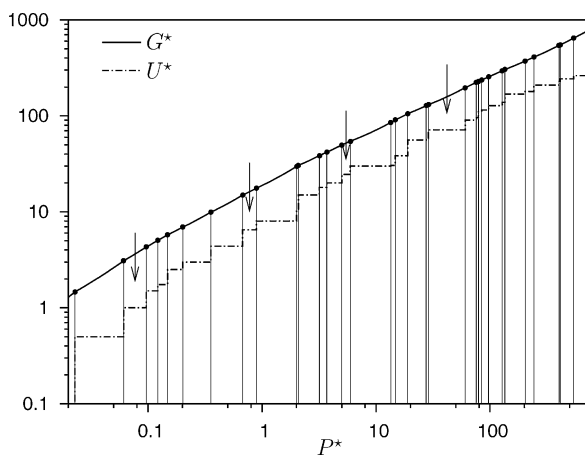


Fig. 2 G^* and U^* as functions of P^* on a double-logarithmic scale for the square-shoulder system, $\lambda = 4.5$. Arrows correspond to states depicted in Fig. 3(a–d).

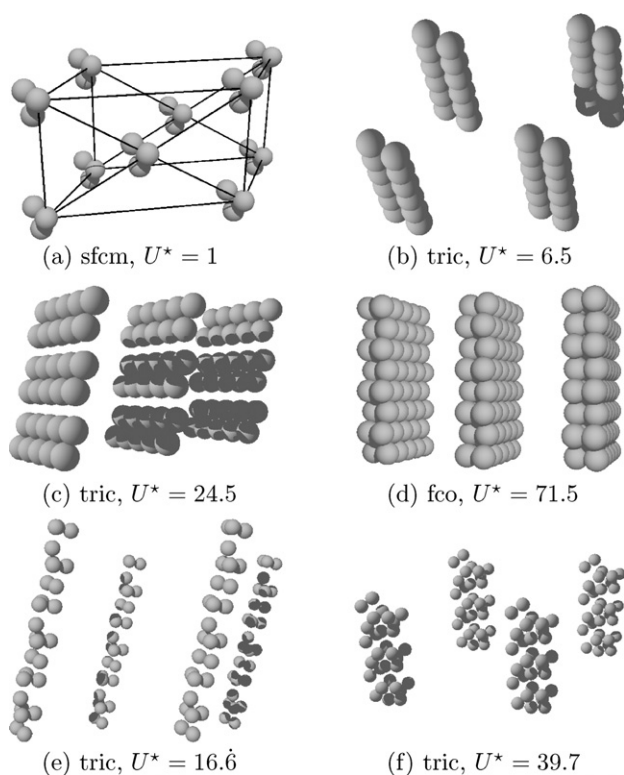


Fig. 3 Selected MECs for the square-shoulder system with $\lambda = 4.5$ [from (a) to (d)] and with $\lambda = 10$ [from (e) and (f)]. MECs (a) to (d) correspond to pressure values indicated by arrows in Fig. 2.

demonstration we have depicted in Fig. 3(a) a typical cluster crystal: the equilateral triangle-shaped clusters populate the lattice positions of a single face centred monoclinic structure. The formation of clusters can also be viewed as a competition between the core- and the corona-contribution to the interaction; we point out that formation of isolated clusters induced by a similar competition has been studied in detail in ref. 26. As the pressure is increased the system develops a new strategy to minimise G by forming columnar structures. Particles aligned in close or direct contact form single or double

stranded columns, which are arranged periodically in space. The inter-columnar spacing is imposed *via* the width of the corona. An example for the columnar phase is given in Fig. 3(b). As the pressure increases further, the columns are squeezed together in one direction, thereby forming lamellae; the transition scenario is depicted in Fig. 3(c). The lamellar structures are realized in a large variety of morphologies. In Fig. 3(d) we show an example for a lamellar phase: here, two hexagonally close-packed, planar layers are in direct contact and form double layers. Finally, under the influence of the increasing pressure, the lamellae merge, creating in this way typical compact structures.

For $\lambda = 10$, the variety of structures is even richer, in total 47 MECs have been identified. The clusters contain more particles and the columns are more complex in their morphology. As a demonstration we depict two of these structures in Fig. 3(e) and (f). However, the sequence of structural archetypes that has already been identified for $\lambda = 4.5$ is maintained.

Taking typical values for the particle diameter (100 nm), the corona-width ($\lambda = 3$), and the shoulder height ($\epsilon = 100k_B T = 2.5$ eV at room temperature) of colloidal particles with core–corona architecture,²² the range for $P^*/\lambda^3 \in [10^{-2}, 10]$ corresponds to $P \in [10^2 \text{Pa}, 10^3 \text{Pa}]$ in experiment. We note that typical experimental pressure values in similar systems are often of the order of ambient pressure ($P \approx 10^5 \text{Pa}$).

The above mentioned transition from clusters to compact structures can be understood on a simple, semi-quantitative level. Generalising the ideas proposed by Glaser *et al.*³ for two dimensional systems, we only consider *aggregates* (*i.e.*, clusters, columns, and lamellae) instead of the individual particles. Assuming an idealised shape for these aggregates (spheres, straight lines, and planes) the inter- and intra-aggregate energy can be calculated. The respective expressions are in some cases rather complex and will be presented elsewhere.²⁵ G^* is then characterised by q^* , the distance between two aggregates, and their spatial extent. Retaining parameters up to first order and minimising G^* with respect to these quantities we obtain the thermodynamic properties of the respective phase. In particular, $(U^* + 1/2)/\lambda^3$ as a function of P^*/λ^3 turns out to be λ -independent and has been plotted, along with the respective results obtained *via* the

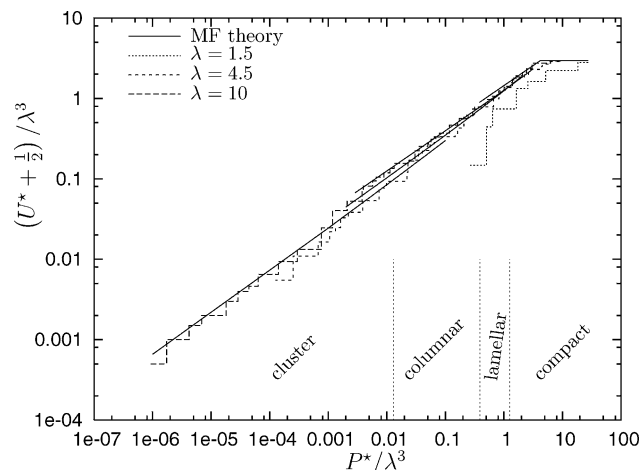


Fig. 4 Scaled energy per particle $(U^* + 1/2)/\lambda^3$ as obtained *via* the MF-theory (full black line) and for the three square-shoulder systems investigated (as labelled) as a function of P^*/λ^3 . The vertical, dotted lines indicate the borders of the four different regimes.

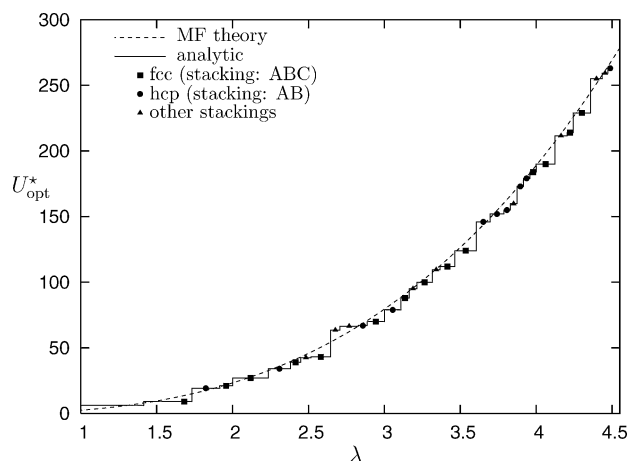


Fig. 5 Minimum number of corona overlaps per particle (U_{opt}^*) and corresponding MECs (as labelled) for close-packed particle arrangements as a function of λ , as obtained *via* analytical considerations and the MF-theory (as labelled). The latter gives $U^*(\varrho^* = \sqrt{2}) = (4\pi\lambda^3/3\sqrt{2}) - (1/2)$.

GA, for all λ -values in Fig. 4. As expected, agreement improves considerably with increasing λ . A detailed analysis of the MECs identified by the GA (in particular for the larger λ 's) reveals, that the MECs populate, according to their aggregate-type, nearly exclusively the respective pressure-range.

Finally, a nice by-product should be mentioned: the well-defined range of the shoulder represents a highly sensitive antenna to discern between competing structures in *close-packed* arrangements. Varying λ from 1 to 4.5, we have identified *via* analytic considerations not only the usual suspects for close-packed scenarios, namely hcp and fcc; also other, more complicated stacking sequences are observed for particular λ -values—*cf.* Fig. 5.

Summarising, our investigations have given *quantitative* evidence about the rich wealth of self-assembly scenarios of soft particles that interact *via* a simple, radially symmetric pair potential: while at high pressure compact structures are dominant, we observe at intermediate and low pressure low-symmetry structures, that include clusters, columns, and lamellae. The simple functional form allows us to fully analytically *understand* the system's self-organisation strategies in such complex scenarios.

The authors are indebted to Dieter Gottwald and Julia Fornleitner (both Wien) for stimulating discussions. Financial support by the Austrian Science Foundation under Proj. Nos. W004, P17823-N08, and P19890-N16 is gratefully acknowledged.

Notes and references

- 1 J. Maddox, *Nature*, 1988, **335**, 201.
- 2 C. Pierleoni, C. Addison, J.-P. Hansen and V. Krakoviack, *Phys. Rev. Lett.*, 2006, **96**, 128302.
- 3 M. Glaser, G. M. Grason, R. D. Kamien, A. Košmrlj, C. D. Santangelo and P. Ziherl, *Europhys. Lett.*, 2007, **78**, 46004.
- 4 A. Campbell, V. J. Anderson, J. S. van Duijneveldt and P. Bartlett, *Phys. Rev. Lett.*, 2005, **94**, 208301.
- 5 A. de Candia, E. Del Gado, A. Fierro, N. Sator, M. Tarzia and A. Coniglio, *Phys. Rev. E*, 2006, **74**, 010403(R).
- 6 A. Stradner, H. Sedgwick, F. Cardinaux, W. C. K. Poon, S. U. Egelhaaf and P. Schurtenberger, *Nature*, 2004, **432**, 492.
- 7 B. Mladek, D. Gottwald, G. Kahl, M. Neumann and C. N. Likos, *Phys. Rev. Lett.*, 2006, **96**, 019901; B. Mladek, D. Gottwald, G. Kahl, M. Neumann and C. N. Likos, *Phys. Rev. Lett.*, 2006, **96**, 045701.
- 8 J. Pannetier, J. Bassasalsina, J. Rodriguez-Carvajal and V. Caignaert, *Nature*, 1990, **346**, 343; J. C. Schön and M. Jansen, *Angew. Chem., Int. Ed. Engl.*, 1996, **35**, 1286.
- 9 S. Goedecker, *J. Chem. Phys.*, 2004, **120**, 9911.
- 10 R. Martoňák, A. Laio and M. Parrinello, *Phys. Rev. Lett.*, 2003, **90**, 075503; R. Martoňák, D. Donadio, A. R. Oganov and M. Parrinello, *Nat. Mater.*, 2006, **5**, 623.
- 11 J. Holland, *Adaptation in Natural and Artificial Systems*, The University of Michigan Press, Ann Arbor, 1975.
- 12 A. Assion, T. Baumert, M. Bergt, T. Brixner, B. Kiefer, V. Seyfried, M. Strehle and G. Gerber, *Science*, 1998, **282**, 919.
- 13 W. P. C. Stemmer, *Nature*, 1994, **370**, 389.
- 14 D. M. Deaven and K. M. Ho, *Phys. Rev. Lett.*, 1995, **75**, 288.
- 15 S. M. Woodley, P. D. Battle, J. D. Gale and C. R. A. Catlow, *Phys. Chem. Chem. Phys.*, 1999, **1**, 2535.
- 16 A. R. Oganov and C. Glass, *J. Chem. Phys.*, 2006, **124**, 244704; A. R. Oganov and C. Glass, *J. Phys.: Condens. Matter*, 2008, **20**, 064210.
- 17 D. Gottwald, C. N. Likos, G. Kahl and H. Löwen, *Phys. Rev. Lett.*, 2004, **92**, 068301.
- 18 J. Fornleitner, F. Lo Verso, G. Kahl and C. N. Likos, *Soft Matter*, 2008, **4**, 480.
- 19 Z. Yan, S. V. Buldyrev, N. Giovambattista, P. G. Debenedetti and H. E. Stanley, *Phys. Rev. E*, 2006, **73**, 051204.
- 20 E. A. Jagla, *J. Chem. Phys.*, 1999, **111**, 8980.
- 21 P. Ziherl and R. Kamien, *J. Phys. Chem. B*, 2001, **105**, 10147.
- 22 Y. Norizoe and T. Kawakatsu, *Europhys. Lett.*, 2005, **72**, 583.
- 23 D. Gottwald, C. N. Likos, G. Kahl and H. Löwen, *J. Chem. Phys.*, 2005, **122**, 074903.
- 24 For two-dimensional simple lattices the parameter space is two-dimensional. Here, the region that corresponds to unphysical, *i.e.*, overlapping particle configurations can be identified rather easily: it is given by infinitely many circles which become for $\varrho\sigma^2$ the so-called Ford circles; the latter represent a super-set of the Apollonian Gasket, *i.e.*, an object with a fractal dimension of 1.3057.
- 25 G. J. Pauschenwein and G. Kahl, unpublished work.
- 26 S. Mossa, F. Sciortino, P. Tartaglia and E. Zaccarelli, *Langmuir*, 2004, **20**, 10756.